IJMTARC – VOLUME – V – ISSUE - 19 – SEPT 2017 ISSN: 2320-1363

Energy Storage System in PV based Charge/Discharge Conditions of Eleven-Level Inverter fedInduction Motor Drive

MERUPO RAMESH
M-tech Student Scholar
Department of Electrical & Electronics Engineering;
SRKR Engineering College, BHIMAVARAM;
WEST GODAVARI (Dt); A.P, India.

Sri K.S.S.PRASADRAJU M.Tech
Assistant Professor
Department of Electrical & Electronics Engineering;
SRKR Engineering College, BHIMAVARAM;
WEST GODAVARI (Dt); A.P, India

Abstract- This paper presents the eleven level inverter with DC source which is used to generate a eleven level output and performance of three phase induction motor is analyzed when connected to PV array DC source (charged and discharged capacitor) is used for getting the output. Multilevel inverter structures have been developed to overcome shortcomings in solid-state switching device ratings so that they can be applied to high voltage electrical systems, inverter output voltage is connected to battery energy stored systems. An asynchronous motor (three-phase) performance characteristics are analyzed. And further the DC source is replaced by a renewable resource such as solar panels, and DC voltage is obtained. Performance characteristics of three-phase asynchronous motor are analyzed with PV array connected. The multilevel voltage source inverters unique structure allows them to reach high voltages with low harmonics without the use of transformers. The proposed inverter uses less number of switches when compared with the conventional multilevel inverter. This concept can be extended to apply for induction motor drive i.e., a 3-Phase eleven Level Inverter for PV cell fed Induction Motor Drive. Simulations have been carried out in MATLAB–Simulink software.

Keywords: Renewable energy sources, multilevel inverters, Energy stored systems, Induction motor.

I.INTRODUCTION

Nowadays renewable energy generation systems are gaining more attraction due to the exhaustive nature of fossil fuel resources and its increased prices. Also the need for pollution free green energy has created a keen interest towards alternate energy sources. Solar power is the most common and available renewable power source to meet our rapidly increasing energy requirements [1-2]. Peak power from the solar PV module is to be tracked for its efficient implementation.

A multilevel inverter not only achieves high powerratings, but also enables the use of renewable energysources. Renewable energy sources such as photovoltaic,wind and fuel cells, which can be easily interfaced to amultilevel inverter system for high power applicationsThe topologies of multilevel inverters are classified in tothree types the Flying capacitor inverter, the Diodeclamped inverter and the Cascaded bridge inverter.[3-4] the output power generated from the solar panels is intermittent in nature and varies with the irradiance level.Hence to make the system more reliable, a battery is included in the system. A bidirectional converter is also used toadjust the flow of power from and into the battery [5-6].Aneleven level inverter is used to convert the dc voltage from thesolar PV array to ac voltage and connect feed to the load.

In this paper a novel topology for single phase five levelinverter is suggested [7]. This topology uses reduced number of switches compared to conventional five level inverter topologies. Multilevel inverters produce a desired output voltage from different levels of direct current voltages as inputs. As the number of levels increases, the synthesized output waveform is staircase wave which approximates a sine wave with more number of steps. Thus the output voltage approaches the desired sinusoidal waveform [8-9].

The main advantages of a multilevel inverter are that they can generate the output voltages with very less THD, can draw input current with very low distortion, lower EMI effects, and lower dv/dt across each switch and can operate at wide range of switching frequencies from fundamental frequency to very high frequency. The most common topologies for multilevel inverters are diode clamped, flying capacitor and cascaded H- bridge multilevel inverter. The paper presents a modified topology for multilevel inverter which uses less number of switches compared to conventional topologies [10-11].

IJMTARC – VOLUME – V – ISSUE - 19 – SEPT 2017 ISSN: 2320-1363

The proposed use of r multilevel inverter haseleven level associated with a power switches[8-9] with the use of single dc source In normal eleven levelinverter use of this t identical dc sources of eleven levels using Multi-level inverter and elevenlevel output is obtained in proposed circuit by using asingle DC source.The same technique is implemented forthree-phase circuit i.e. by using single DC source [12-13].

Anasynchronous motor (three-phase) is connected as loadand its performance characteristics are analyzed. Andfurther the DC source is replaced by a renewable resourcesuch as solar panels, fuel cell etc. and DC voltage isobtained. Performance characteristics of three-phase[14] asynchronous motor are analyzed with PV arrayconnected. To develop the model of proposed reduced number of multilevelinverter, a simulation is done based onMATLAB/SIMULINK software.

II. PROPOSED BESS CONTROL SCHEME

In order to afford operation of the micro-grid in both grid-connected and islanding states, the battery control system should be able to regulate the DC bus voltage and provide a stable grid operation. The primary source of power generation for the studied DC micro-grid is considered to be of renewable ones, which are often controlled to operate at MPPT while the battery meets the sensitive load demand to maintain a continuous supply of power in case of fluctuations in the main grid or during islanding operation. Different operating modes are considered for the DC micro-grid, which are summarized in Table 1. In mode I, the DC micro-grid is connected to the main grid, the RES is working in MPPT, BESS in charging or floating state, while the DC bus voltage and power balance are controlled by the grid-side voltage-source converter (GS-VSC). Modes II and III correspond to the islanding state of the micro-grid where the RES is operating in MPPT and the insufficient/surplus power is balanced by discharging/charging of the BESS. In these two modes, the BESS is responsible for voltage regulation. In mode IV, the micro-grid is also in islanding state and the required power is larger than the total maximum power of RES and BESS, or the battery is in a low SoC. Consequently, in order to maintain the system stability load shedding is required.

a) Battery modelling

A proper charge–voltage model is essential in order to study the battery behavior during charge and discharge conditions. Owing to the non-linear characteristic of battery, its proper representation in the controller is a challenge. In a renewable-based micro-grid with an intermittent power generation profile, it is imperative to consider the dynamical behavior of batteries. Different models for simulating battery behavior with different degrees of complexity and precision are available. These models can be categorized into three groups; electrochemical, mathematical and electrical models.

Electrochemical modelscharacterize the battery mechanisms by a set of differential equations. Such models are too complex for real-time control purposes and are useful for evaluating actual conditions of the battery. In mathematical models, the performance of the battery is simply described by some empirical equations with no particular practical meaning. Electrical models represent the battery behavior with basic electrical elements, such as voltage and current sources, resistors and capacitors. Although this kind of model ignores some chemical reactions in the battery such as stratification, but it is more intuitive, relatively simple and adequate for investigating the control system that makes it a widely effective model for control simulation purposes. Various kinds of such electrical models have been proposed in the literatures. The simplest electrical model of a battery contains an ideal voltage source in series with a constant internal resistance. Another commonly used model is the Thevenin equivalent model, which consists of an ideal no-load battery voltage, series internal resistance in series with a parallel combination of over-voltage resistance and capacitance. In the Thevenin equivalent model, transient behavior of the battery can be simulated.

However, this model just considers battery discharging mode, and the charging and run-time behavior of the battery cannot be simulated. Models that are more realistic have been proposed to take into account the non-linear parameters and the battery dynamical behavior. A dynamic battery model for lead-acid batteries is proposed. This electrical model characterizes different working zones for battery run-time, that is, saturation, overcharge, charge, discharge and over-discharge zones shown in Fig.1. Results show that this model can satisfactorily demonstrate the behavior of batteries during the charge/discharge processes; however, the transient performance of battery cannot be investigated through such models.

Table1 DC micro-grid operating modes

IJMTARC – VOLUME – V – ISSUE - 19 – SEPT 2017 ISSN: 2320-1363

Mode	Micro-grid state	PV state	BESS state	GS-VSC
I	grid-connected	MPPT	charging/off	inverting/ rectifying mode
II	islanding	MPPT	discharging/ off	disconnected
III	islanding	MPPT	charging/off	disconnected
IV	islanding	MPPT	limited	disconnected

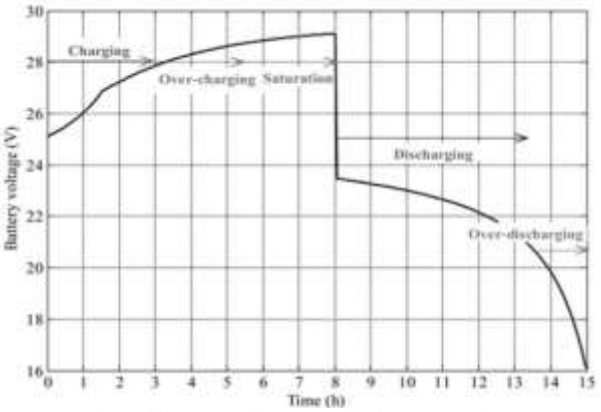

Fig.1 Different working zones for battery run-time

According to the above discussion, for the battery modelling and in order to apply a proper model for both charging and discharging processes, a combinatory model based on the run-time based and Thevenin model is modified and used in this paper in order to simulate charge/ discharge behavior of the battery in the proposed control strategy. The equivalent circuit model is depicted in Fig.2.

In this model, the voltage source Vg represents the battery open circuit voltage, Rsb models the internal resistance of the battery, which contains the effect of operating point (I, SoC). Owing to the cost consideration, higher availability and ease of manufacturing, lead-acid battery is still widely used in different applications such as micro-grids. The capacity-based normalized forms of the equations for lead-acid battery are as follows:

Discharge zone

$$V_g = 2.085 - 0.12(1 - \mathrm{SoC}) \quad (1)$$

$$R_{sb} = \frac{I}{C_{10}}\left(\frac{4}{1+I^{1.3}} + \frac{0.27}{\mathrm{SoC}^{1.5}} + 0.02\right) \quad (2)$$

Where $\mathrm{SoC} = (1 - (Q/C))$, $Q = I \cdot t$. C_{10} is the nominal capacity (in ampere-hours) after a 10h charging?

Charge zone

$$V_g = 2 + 0.16(\mathrm{SoC}) \quad (3)$$

$$R_{sb} = \frac{I}{C_{10}}\left(\frac{6}{1+I^{0.86}} + \frac{0.48}{(1-\mathrm{SoC})^{1.2}} + 0.036\right) \quad (4)$$

Furthermore, the RC network (Rtb, Ctb), similar to that in Thevenin model, simulates the transient response. The parameters are

$$R_{tb} = 0.086\, I^{-0.67}\left(70.3 - 11.66\, V_{oc} + 0.49\, V_{oc}^2\right) \quad (5)$$

$$C_{tb} = \left(326.5\, I^{-1.1}\, R_{tb}\right)^{-1} \quad (6)$$

b) Control algorithm for the battery

According to the operating modes presented in Table 1, the battery is expected to be charged or discharged under different grid operating modes. Efficient use of the battery and its effective life highly depends on the battery charge and discharge method.

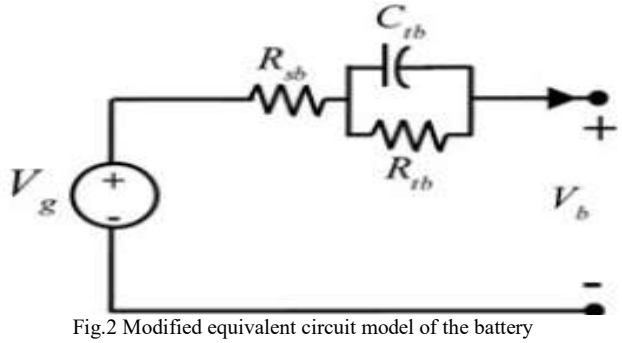

Fig.2 Modified equivalent circuit model of the battery

A commonly applied charging strategy is based on on/off control. However, this control method is not suitable for micro-grid applications since it causes prolonged charging process. Furthermore, in the islanding mode and during the off time, no energy is transferred to the battery. As a result, the accessible renewable energy may not be stored properly and the voltage regulation task cannot be carried out by this control strategy in case of battery charging. Another proposed method for battery charging is by means of the SoC estimation. However, accurate estimation of the SoC and its implementation is complicated. In, a battery charging strategy is developed for PV applications in which the charging process is fulfilled in three stages as shown in Fig.3.

During the first stage, the battery is charged under constant current according to the nominal battery charging current. When the battery voltage reaches the gassing voltage, the second stage begins and the charging is completed via constant voltage charging mode. The third stage corresponds to the floating charge where the battery is fully charged. It has been shown that this algorithm can be effectively used for battery charging in

IJMTARC – VOLUME – V – ISSUE - 19 – SEPT 2017 ISSN: 2320-1363

renewable energy systems. This algorithm is implemented in the proposed control system for charging the battery. However, since the battery is planned to regulate the DC voltage during different operating modes, it is required to disregard this charging algorithm in the case where the micro-grid is islanded and the generated renewable energy is in excess of the demanded load. In such operating condition, the controller is designed to charge the battery in a constant voltage mode while keeping the DC bus voltage regulated in the permissible range.

Besides the charging, the discharging control of the battery is also important in order to smoothly regulate the DC voltage by the control of power discharge in accordance with the demanded load. Furthermore, the control system is designed to limit the battery discharge current and avoid over-discharging, when SoC of the battery is beneath the tolerable value, or over-loading, when the demanded power is more than battery maximum power. In such cases, a load-shedding strategy should be followed. The load shedding and power management strategies are reviewed.

c) Proposed battery charge/discharge control scheme

A grid interface is required for the connection of battery to the DC micro-grid. One of the most flexible methods for the superior performance of battery is to connect it by a proper DC/DC converter. A bi-directional buck-boost DC/DC converter shown in Fig.4 is used in the current study for the battery interface. In this circuit L, RL represents the converter input filter and Co, Ro are the output filter. Under different micro-grid conditions, the battery operates at charging, discharging or floating modes, and the modes are managed according to the DC bus voltage condition at the point of BESS coupling.

The proposed control strategy regulates the converter input voltage (or equally the battery terminal voltage) during the charging process. This approach allows controlling the battery charge/discharge and protecting over-charge/discharge with no need to estimate the battery SoC that is usually a difficult task. In case of voltage control mode, for example, in micro-grid islanding operation, an external voltage control loop adjusts the converter reference input voltage to achieve the grid voltage regulation.

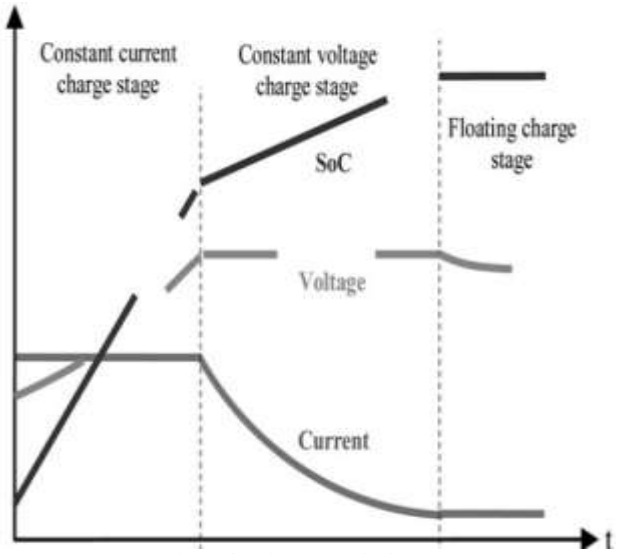

Fig.3 Charging stages for battery

The overall block diagrams of the proposed control topologies for the BESS are shown in Fig.5. The DC/DC boost converter employs the peak current-mode (PCM) control with slope compensation to control the input voltage. The PCM control is a two-loop control system: a voltage loop with an additional inner current loop that monitors the inductor current (or equally the battery current) and compares it with its reference value (I_{bat}^{ref})which is generated by the battery voltage controller shown in Fig.6. The battery current limiter block limits the current to the maximum battery charging current (I_c^{max})and discharging current (I_{dc}^{max}) values. In the proposed control strategy, a combined outer voltage loop is added to generate the converter reference voltage command (V_{bat}^{ref}) by means of considering both the battery voltage set point (V_{bat}^{sp})and the reference grid voltage control value(V_{VC}^{ref}). Converter input voltage is regulated to control the battery SoC or the output DC voltage when needed. The grid voltage

IJMTARC – VOLUME – V – ISSUE - 19 – SEPT 2017 ISSN: 2320-1363

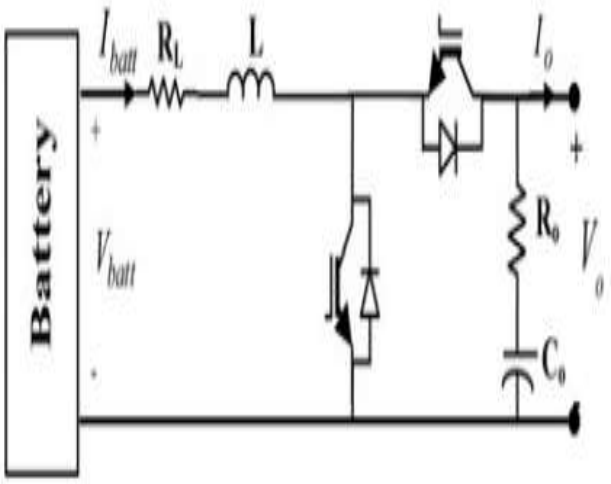

Fig.4 Bidirectional buck-boost battery converter

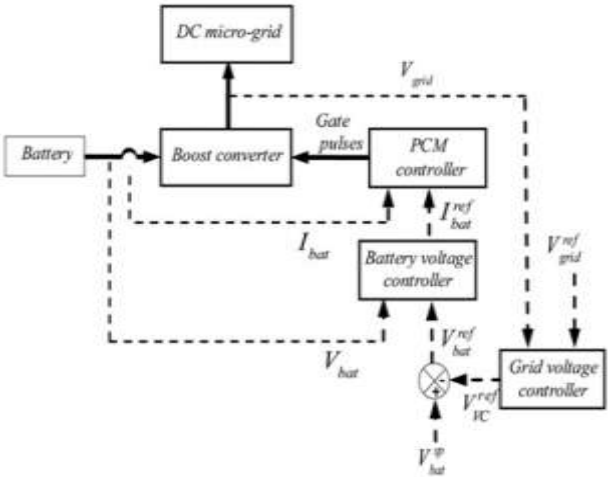

Fig.5 Block diagram of the proposed control topologies for BESS

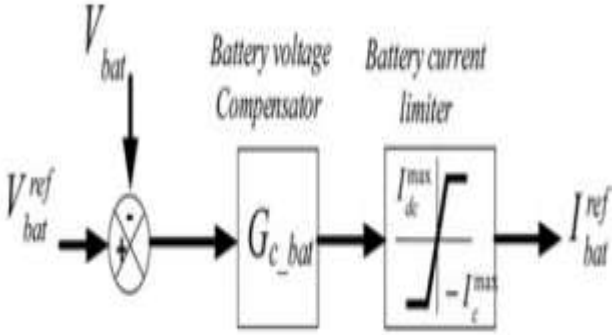

Fig.6 Block diagram of the battery voltage controller in Fig.5

Controller, shown in Fig.7, compares the grid voltage (V_{grid}) with the islanded grid reference voltage ($\tilde{V}_{island}^{ref}$). $\tilde{V}_{island}^{ref}$ is selected to be greater than the maximum value of the controlled grid voltage by GS-VSC.

Therefore, in the grid-connected mode $V_{grid} - \tilde{V}_{island}^{ref} \leq 0$ and the generated signal will be limited to zero by the negative limiter block. In this case, the battery voltage controller loop controls the battery charging process. On the other hand, in case of islanded micro-grid operation with insufficient renewable power generation, the grid voltage control loop will go positive and shifts V_{bat}^{ref} by controlling V_{VC}^{ref} and the insufficient power will be supplied by controlling the discharge of the battery. $\tilde{V}_{island}^{ref}$ Is generated according to the battery output voltage which resembles the SoC. When the battery voltage (V_{bat}) is above the minimum acceptable battery voltage(V_{bat}^{min}), that corresponds to the secure SoC, the relay block sets the output to V_{grid}^{ref}. On the other hand, if $V_{\text{bat}} < V_{bat}^{min}$, the battery is in low SoC and there is not enough charge for supplying the total load. In this case, $\tilde{V}_{island}^{ref}$ is set to the shedding voltage (V_{shed}) in order to trigger the load-shedding system. Accordingly, some unimportant loads in the micro-grid will be shed and energy for sensitive ones will be saved. An anti-windup control is also added to compensate the saturation of the control variable, which is commonly caused in a controller implementation and results in integral windup. The combination of these two voltage control loops is exploited to instantaneously balance the system power and controlling the grid voltage in required operating modes. Moreover, when the available maximum discharge power of the battery is less than the demanded power, the load-shedding system will trip the required amount of the load to avoid over-discharge of the battery.

III. SMALL SIGNAL MODELLING AND CONTROLLER DESIGN

According to the battery equivalent circuit model in Fig.2 and using the averaging method for the DC/DC converter, the BESS model can be expressed by the following equations

$$\frac{di_L}{dt} = \frac{1}{L}\left[-\left(R_L + R_{sb}\right)i_L + (1-d)v_o - v_{tb} + v_g\right] \quad (7)$$

$$\frac{dv_o}{dt} = \frac{1}{C_o}\left[(1-d)\,i_L - i_o\right] \quad (8)$$

IJMTARC – VOLUME – V – ISSUE - 19 – SEPT 2017 ISSN: 2320-1363

$$\frac{dv_{tb}}{dt} = \frac{1}{C_{tb}}\left[i_L - \frac{1}{R_{tb}}v_{tb}\right] \quad (9)$$

And battery output voltage is

$$v_b = v_g - R_{sb}i_L - v_{tb} \quad (10)$$

The averaged small-signal state-space model of the BESS is derived by the linearization of (7) – (9), and by taking the inductor current ($\hat{\imath}_L$), output voltage ($\hat{v}_o$)and the capacitor voltage in the battery model ($\hat{v}_{tb}$)as the state variables and duty cycle $\hat{d}$ and output current $\hat{\imath}_o$ as the inputs. The simplified small-signal block diagram model of the system is illustrated in Fig.8. Related transfer functions are found using the state-space model.

In Fig.8, Fm, Fv and Fo model the peak-current mode controller with slope compensation. These parameters are defined as follows

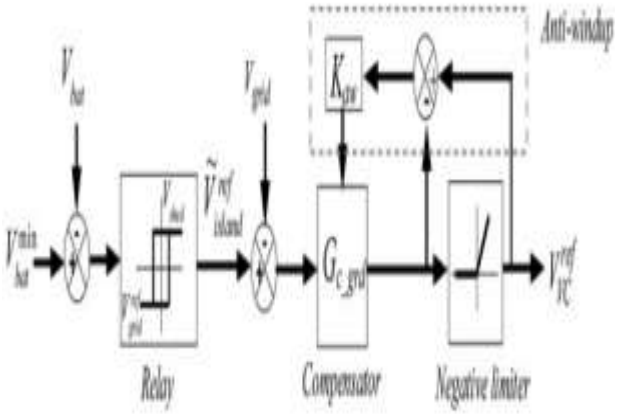

Fig.7 Block diagram of the grid voltage controller in Fig.5

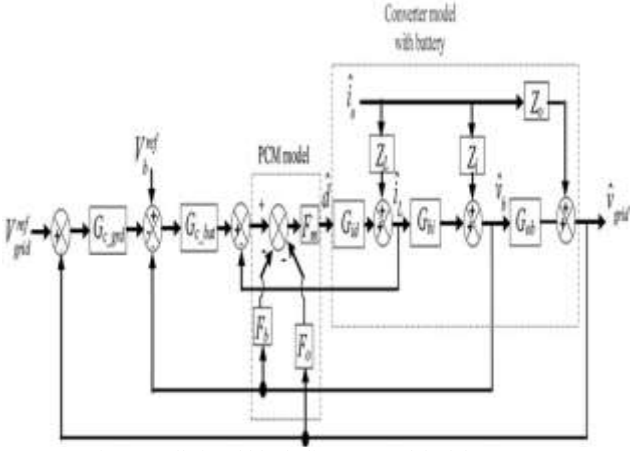

Fig.8 Small signal block diagram model of the BESS

$$F_o = -\frac{D'^2 T_s}{2L} \quad (11)$$

$$F_b = \frac{D^2 T_s}{2L} \quad (12)$$

$$F_m = \frac{1}{M_a T_s} \quad (13)$$

Where Ts is the period of gate-pulses and Ma is the slope of the artificial ramp for the slope compensation. Since the model parameters depend on the state of charge and the battery current, it is required to analyze the model for the worst operating condition in designing the battery controller. The important role of the BESS is in discharging mode for regulating the grid voltage during occurrence of different disturbances. However, the maximum charge current condition has a lower bandwidth. Therefore the control system is designed for the maximum discharge current and simulated for other operating points to verify the controller performance.

IV. OPERATION AND MODELLING OF DC MICRO-GRID

a) Renewable-energy-based DC micro-grid Characteristics

The previous section dealt with the modelling and control of BESS. In order to evaluate the performance of the storage system in a renewable-energy-based DC micro-grid, a simple micro-grid schematically shown in Fig.3.9 is selected as the study case. The micro-grid contains PV system as a renewable energy along with the BESS described in previous sections. The micro-grid is also connected to the main grid via a VSC. The function of GS-VSC is to regulate the DC-link voltage during grid-connected mode. A two-level VSC is used to link DC and AC grids. Current-mode control approach is exploited for real/reactive power control at AC side. Thus, the amplitude and the phase angle of the VSC terminal voltage are controlled in a dq rotating reference frame. The DC-link voltage control is achieved through the control of real power component. DC voltage dynamics can be formulated based on the principle of power balance, as

IJMTARC – VOLUME – V – ISSUE - 19 – SEPT 2017 ISSN: 2320-1363

$$\frac{\mathrm{d}}{\mathrm{d}t}\left(\tfrac{1}{2}C \times V_{\mathrm{DC}}^2\right) = P_{\mathrm{dc}} - P_{\mathrm{ac}} \quad (14)$$

$$P_{\mathrm{dc}} = V_{\mathrm{DC}} \times i_{\mathrm{grid}}^{\mathrm{DC}} \quad (15)$$

A DC/DC converter is also used for the connection of PV arrays to the micro-grid. A general perturbation-and-observe MPPT method along with the control system is implemented for the PV system in the current study.Composite DC loads including constant power and constant impedance terms are modelled to verify the stable operation of the system for different micro-grid operating modes.

b) Power management strategy

In a real grid, there may be multiple of sources dispersed throughout the grid, thus a distributed power management strategy is needed to coordinate the sources/storages effectively. The modified DC-bus signaling method is used in this paper to coordinate the proposed battery controller with the PV generation system and to obtain the power balance and stable operation of DC micro-grid under various generation or load conditions.

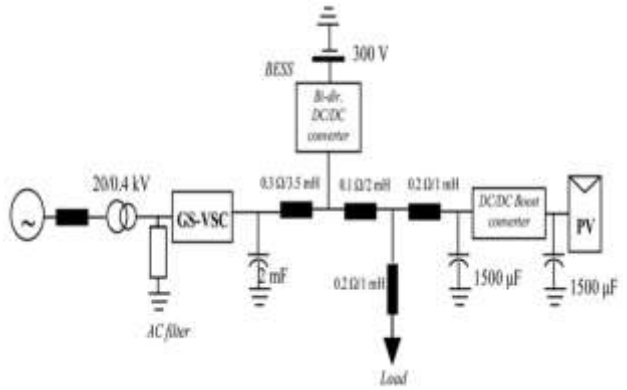

Fig.9 Schematic diagram of the simulated DC micro-grid

V. INDUCTION MOTOR

An asynchronous motor type of an induction motor is an AC electric motor in which the electric current in the rotor needed to produce torque is obtained by electromagnetic induction from the magnetic field of the stator winding. An induction motor can therefore be made without electrical connections to the rotor as are found in universal, DC and synchronous motors. An asynchronous motor's rotor can be either wound type or squirrel-cage type.

Three-phase squirrel-cage asynchronous motors are widely used in industrial drives because they are rugged, reliable and economical. Single-phase induction motors are used extensively for smaller loads, such as household appliances like fans.

Although traditionally used in fixed-speed service, induction motors are increasingly being used with variable-frequency drives (VFDs) in variable-speed service. VFDs offer especially important energy savings opportunities for existing and prospective induction motors in variable-torque centrifugal fan, pump and compressor load applications. Squirrel cage induction motors are very widely used in both fixed-speed and variable-frequency drive (VFD) applications. Variable voltage and variable frequency drives are also used in variable-speed service.

In both induction and synchronous motors, the AC power supplied to the motor's stator creates a magnetic field that rotates in time with the AC oscillations. Whereas a synchronous motor's rotor turns at the same rate as the stator field, an induction motor's rotor rotates at a slower speed than the stator field. The induction motor stator's magnetic field is therefore changing or rotating relative to the rotor. This induces an opposing current in the induction motor's rotor, in effect the motor's secondary winding, when the latter is short-circuited or closed through external impedance. The rotating magnetic flux induces currents in the windings of the rotor; in a manner similar to currents induced in a transformer's secondary winding(s). The currents in the rotor windings in turn create magnetic fields in the rotor that react against the stator field. Due to Lenz's Law, the direction of the magnetic field created will be such as to oppose the change in current through the rotor windings. The cause of induced current in the rotor windings is the rotating stator magnetic field, so to oppose the change in rotor-winding currents the rotor will start to rotate in the direction of the rotating stator magnetic field. The rotor accelerates until the magnitude of induced rotor current and torque balances the applied load. Since rotation at synchronous speed would result in no induced rotor current, an induction motor always operates slower than synchronous speed.The difference, or "slip," between actual and synchronous speed varies from about 0.5 to 5.0% for standard Design B torque curve induction motors.

The induction machine's essential character is that it is created solely by induction instead of being separately excited as in synchronous or DC machines or being self-magnetized as in permanent magnet motors.

IJMTARC – VOLUME – V – ISSUE - 19 – SEPT 2017 ISSN: 2320-1363

For rotor currents to be induced the speed of the physical rotor must be lower than that of the stator's rotating magnetic field (n_s); otherwise the magnetic field would not be moving relative to the rotor conductors and no currents would be induced. As the speed of the rotor drops below synchronous speed, the rotation rate of the magnetic field in the rotor increases, inducing more current in the windings and creating more torque. The ratio between the rotation rate of the magnetic field induced in the rotor and the rotation rate of the stator's rotating field is called slip. Under load, the speed drops and the slip increases enough to create sufficient torque to turn the load. For this reason, induction motors are sometimes referred to as asynchronous motors. An induction motor can be used as an induction generator, or it can be unrolled to form a linear induction motor which can directly generate linear motion.

Synchronous Speed:

The rotational speed of the rotating magnetic field is called as synchronous speed.

$$Ns = \frac{120 \times f}{P} \quad (RPM) \tag{16}$$

Where, f = frequency of the supply

P = number of poles

Slip:

Rotor tries to catch up the synchronous speed of the stator field, and hence it rotates. But in practice, rotor never succeeds in catching up. If rotor catches up the stator speed, there won't be any relative speed between the stator flux and the rotor, hence no induced rotor current and no torque production to maintain the rotation. However, this won't stop the motor, the rotor will slow down due to lost of torque, and the torque will again be exerted due to relative speed. That is why the rotor rotates at speed which is always less the synchronous speed.

The difference between the synchronous speed (Ns) and actual speed (N) of the rotor is called as slip.

$$\% \text{ slip} \quad s = \frac{Ns - N}{Ns} \times 100 \tag{17}$$

VI. MATLAB/SIMULINK RESULTS

Case: 1

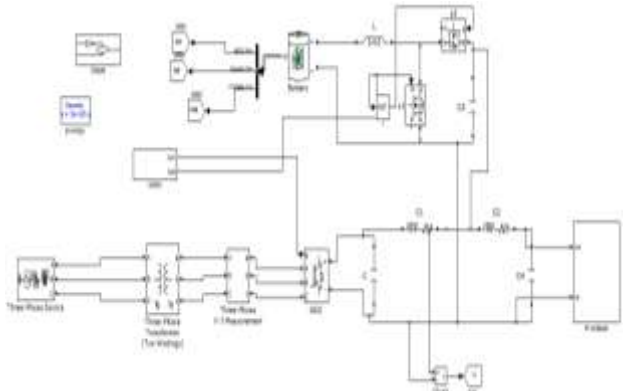

Fig. 1 Schematic diagram of the simulated DC micro-grid

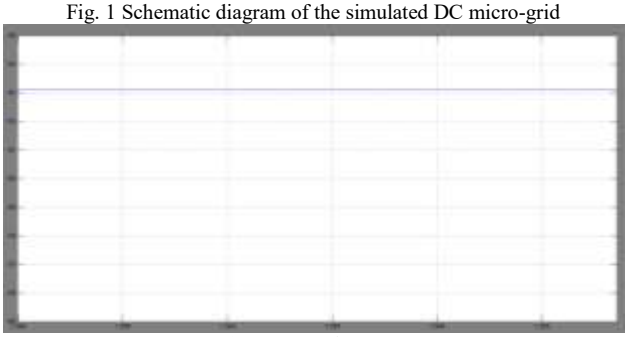

(a) Battery voltage (V)

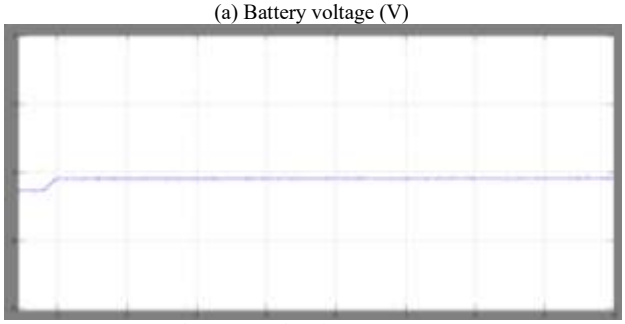

(b) Battery charging current (A)

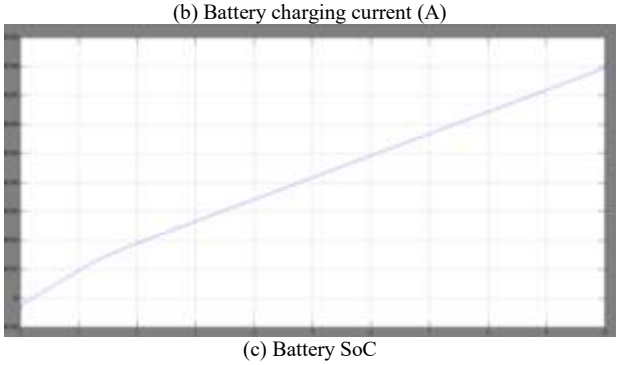

(c) Battery SoC

Fig.2 Battery charging process in grid-connected mode (Case 1)

Case: 2

IJMTARC – VOLUME – V – ISSUE - 19 – SEPT 2017 ISSN: 2320-1363

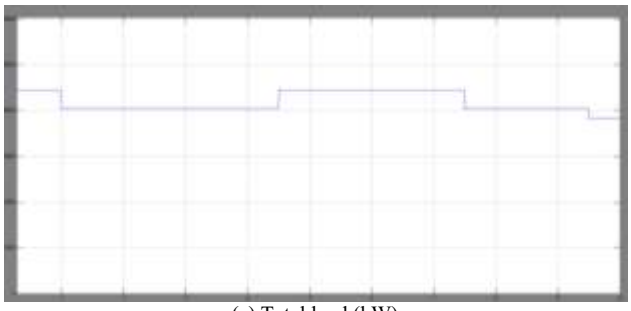

(a) Total load (kW)

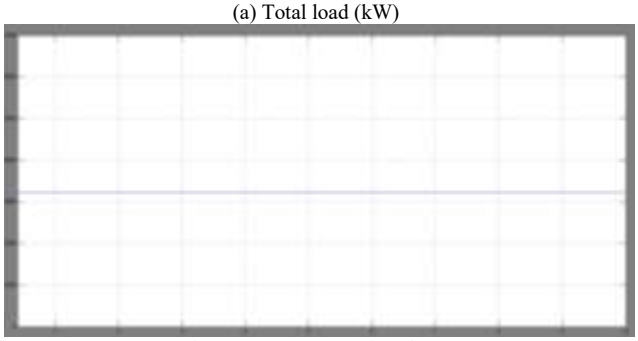

(b) PV power generation (kW)

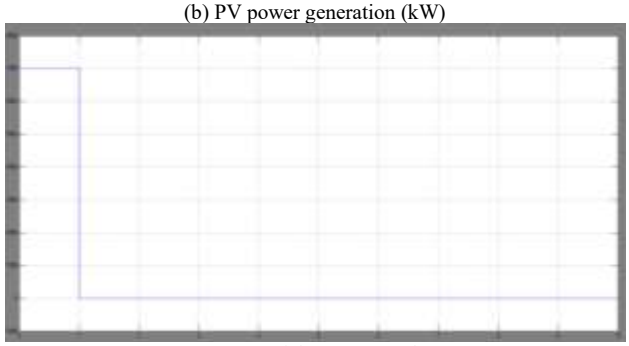

(c) Power of the GS-VSC (kW)

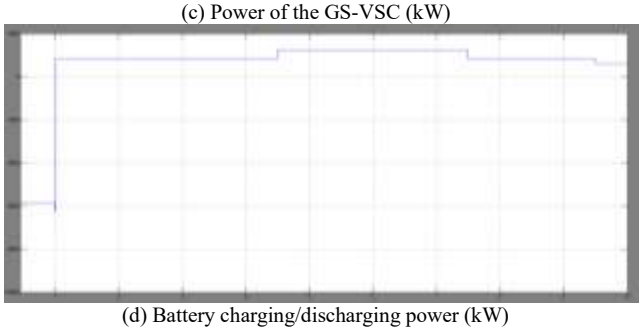

(d) Battery charging/discharging power (kW)

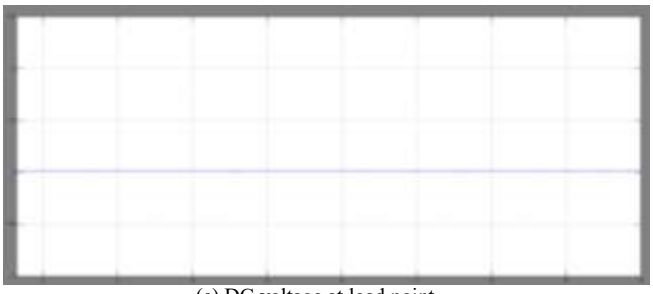

(e) DC voltage at load point

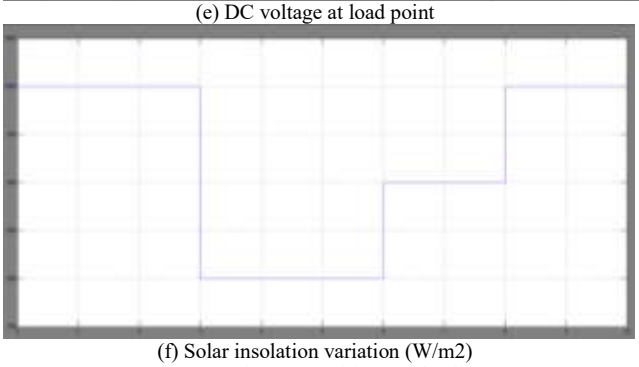

(f) Solar insolation variation (W/m2)

Fig. 3 System operation in transition to islanding (Case 2)

Case: 3

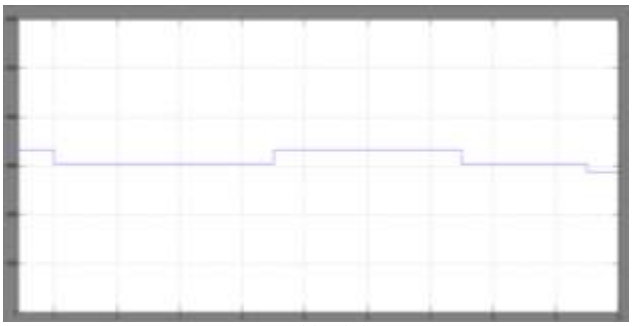

(a) Total load (kW)

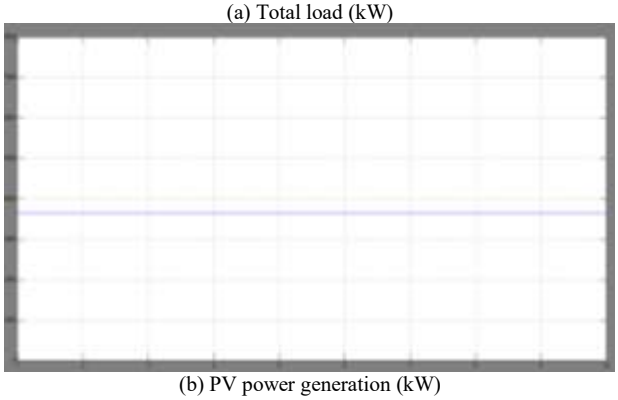

(b) PV power generation (kW)

IJMTARC – VOLUME – V – ISSUE - 19 – SEPT 2017 ISSN: 2320-1363

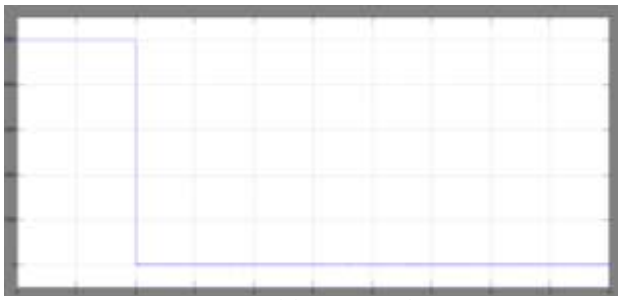

(c) Power of the GS-VSC (kW)

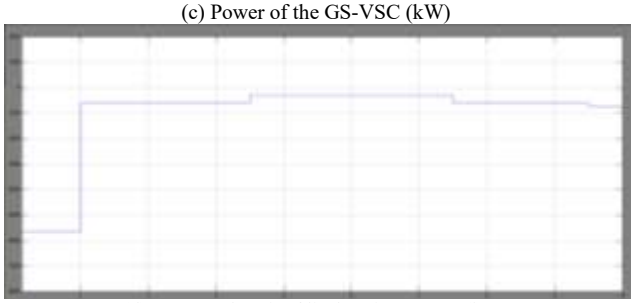

(d) Battery charging/discharging power (kW)

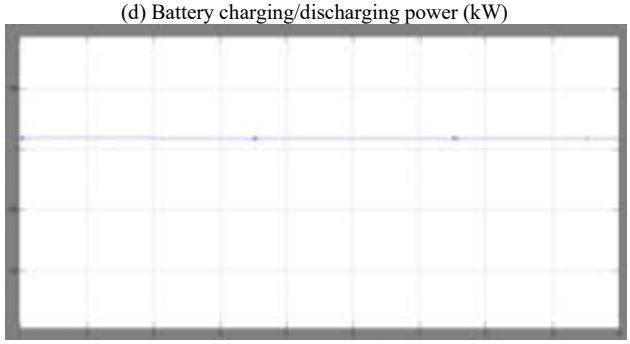

(e) DC voltage at load point

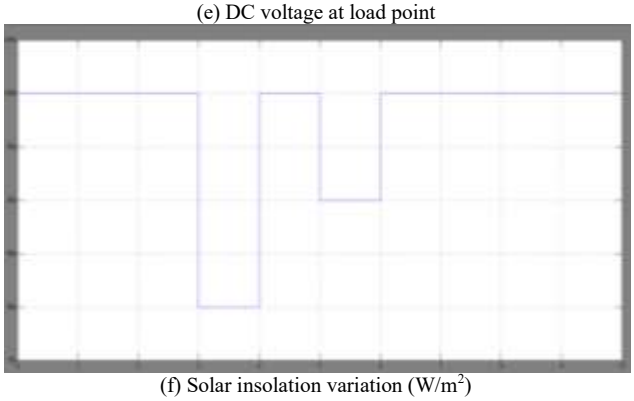

(f) Solar insolation variation (W/m^2)

Fig.4 System operation in transition to islanding (Case 3)

Case: 4

(a) Total load (kW)

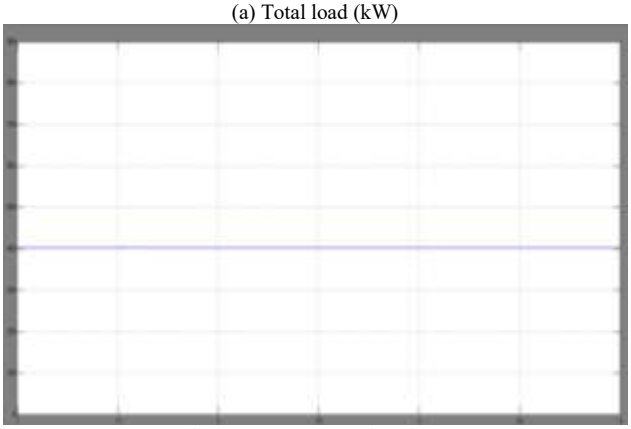

(b) PV power generation (kW)

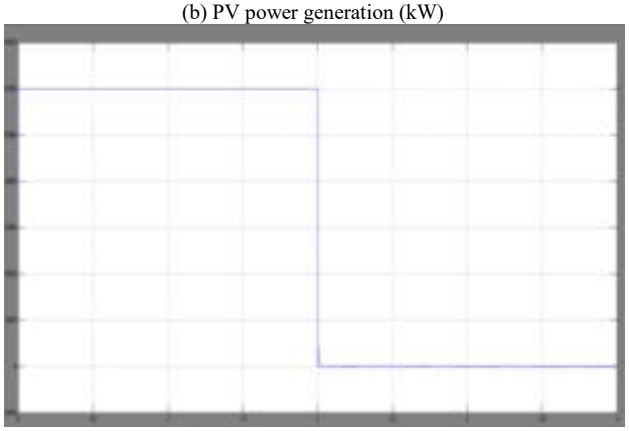

(c) Power of the GS-VSC (kW)

IJMTARC – VOLUME – V – ISSUE - 19 – SEPT 2017 ISSN: 2320-1363

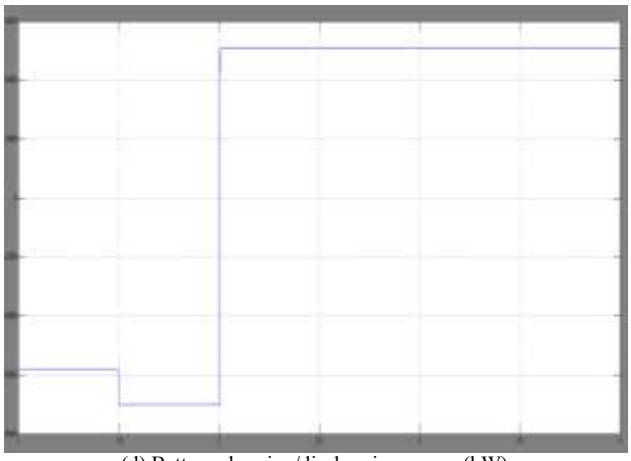

(d) Battery charging/discharging power (kW)

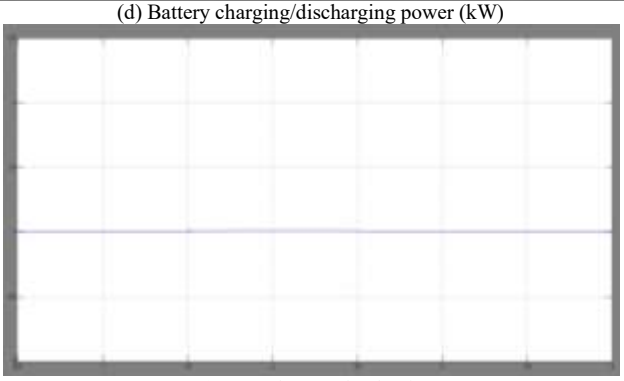

(e) DC voltage at load point

Fig.5 System operation in transition to islanding (Case 4)

Case: 5

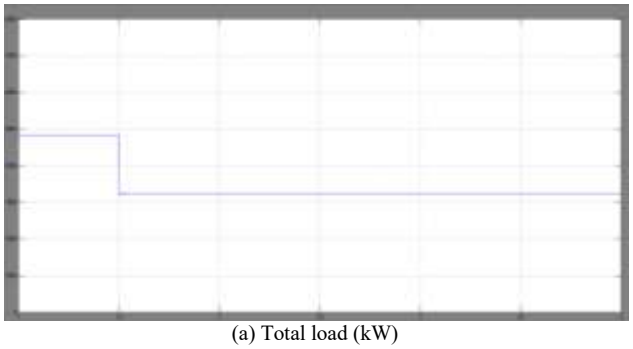

(a) Total load (kW)

(b) PV power generation (kW)

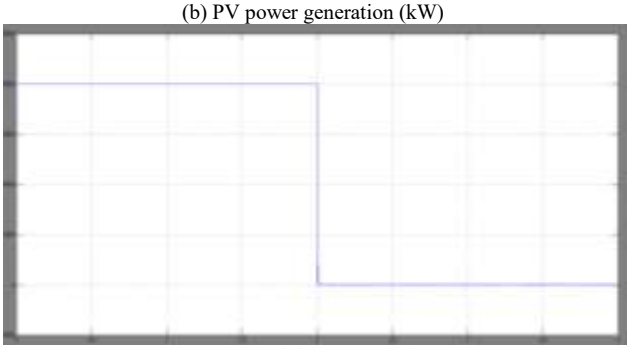

(c) Power of the GS-VSC (kW)

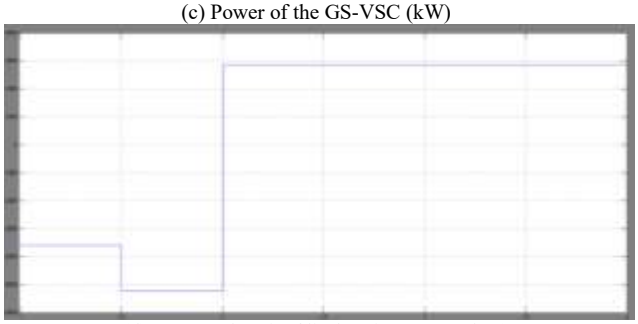

(d) Battery charging/discharging power (kW)

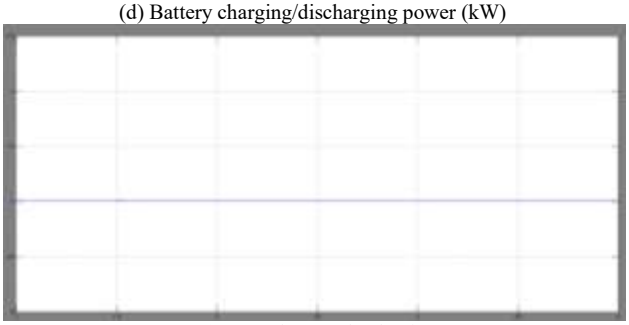

(e) DC voltage at load point

Fig.6 System operation in transition to islanding (Case 5)

IJMTARC – VOLUME – V – ISSUE - 19 – SEPT 2017 ISSN: 2320-1363

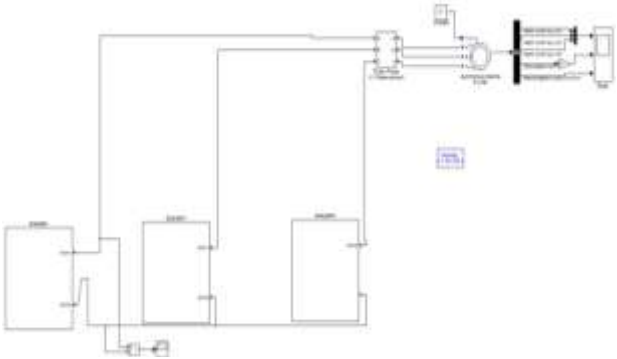

Fig.7 MATLAB/SIMULINK model of three-phase inverter with induction motor

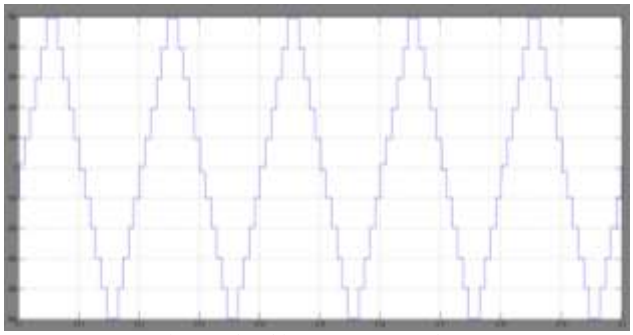

Fig.8 11-level inverter output voltage

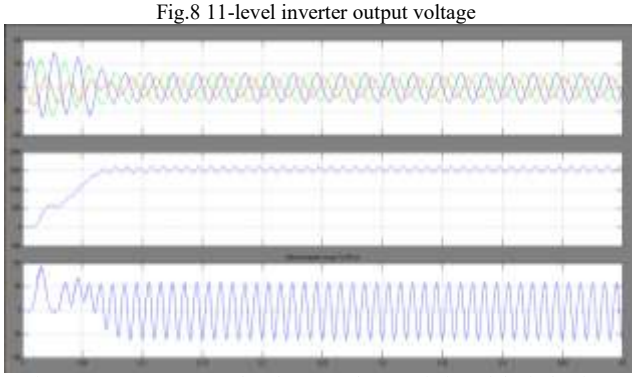

Fig.9 stator current, speed and torque characteristics of the induction motor

VII. CONCLUSION

This paper presented an eleven-level multilevel Inverter, which uses single DC source and PVsystem as DC source and connected to three phaseinduction motor is used as load to observe theperformance characteristics of the motor. The proposedMultilevel Inverter fed Induction Motor. DCvoltage levels are used as a communication link in order tocoordinate the sources and storages in the system and actsas a control input for the operating mode adaptation duringdifferent operating conditions.Stability of dc-dc converter, found that designed dc-dc converter isfully stable. Based on MATLAB based simulations, it is found that proposed advanced powerelectronics based interface is suitable to drive the induction motor.Their speed and torqueare compared. We have observed that the performance of the induction motor drive improveswith increase in voltage level of the inverter.

REFERENCES

[1]. J. S. Lai and F. Z. Peng, “Multilevel converters – A new breed of power converters,” *IEEETrans. Ind. Applicat.*, vol. 32, pp. 1098–1107, May/June 1996.

[2]. J. Rodriguez, J.-S. Lai, and F. Z. Peng, "Multilevel inverters: a survey of topologies, controls,and applications," *IEEE Trans. Ind. Electron.*, vol. 49, pp. 724-738, 2002.

[3]. L. M. Tolbert, F. Z. Peng, and T. G. Habetler, "Multilevel converters for large electricdrives," *IEEE Trans. Ind. Applicat.*, vol. 35, pp. 36-44, 1999.

[4]. M. F. Escalante, J. C. Vannier, and A. Arzande “Flying Capacitor Multilevel Inverters andDTC Motor Drive Applications,” IEEE Transactions on Industry Electronics, vol. 49, no. 4,Aug. 2002, pp. 809-815.

[5]. L. M. Tolbert, F. Z. Peng, “Multilevel Converters as a Utility Interface for RenewableEnergy Systems,” in Proceedings of 2000 IEEE Power Engineering Society SummerMeeting, pp. 1271-1274.

[6] Masters, Gilbert M. Renewable and EfficientElectric Power Systems John Wiley &Sons Ltd, 2004.

[7] D. Zhong B. Ozpineci, L. M. Tolbert, J. N.Chiasson, “Inductor less DC-AC cascaded HBridge multilevel boost inverter for electric/hybrid electric vehicle applications,” IEEE IndustryApplications Conference, Sept. 2007, pp. 603-608.

[8] Shagar Banu M, Vinod S, Lakshmi.S, “Design of DC-DC converter for hybrid wind solar energy system”,2012 International conference onComputing, Electronics and Electrical Technologies.

[9] Thanujkumar.Jala, G. Srinivasa Rao,” A novel nine level grid connected inverter for photovoltaic system” International journal of modernEngineering Research, vol.2, issue.2, March-April 2012, Page(s): 154-159.

[10] Faete Filho, Yue cao, Leon M.Tolbert, “11 level cascaded H bridge grid tied inverter interface with solar panels”, Publication year: 2010

[11] Kuo-Ching Tseng and Chi-Chih Hung “High step-up High-Efficiency Interleaved Converter with Voltage Multiplier Module for Renewableenergy system”, IEEE Trans. Ind.Electron., vol. 61, no. 3, pp. 0278–0046, March. 2014.

[12] Y. P. Hsieh, J. F. Chen, T. J. Liang, and L. S. Yang, “Novel high step-up DC–DC converter for distributed generation system,” IEEE Trans.Ind.Electron., vol. 60, no. 4, pp. 1473–1482, Apr. 2013.

[13]. In-Dong Kim, Eui-Cheol Nho,, Heung-Geun Kim, , and Jong Sun Ko,. ‘A GeneralizedUndeland Snubber for Flying Capacitor Multilevel Inverter and Converter‟.IEEE transactionson industrial electronics, vol. 51, no. 6, December 2004.

[14]. E. Cengelci, S. U. Sulistijo, B. O. Woom, P. Enjeti, R. Teodorescu, and F. Blaabjerg, “ANew Medium Voltage PWM Inverter Topology for Adjustable Speed Drives,” in Conf. Rec.IEEE-IAS Annu. Meeting, St. Louis, MO, Oct. 1998, pp. 1416-1423.

IJMTARC – VOLUME – V – ISSUE - 19 – SEPT 2017 ISSN: 2320-1363